Lithium-Ion Capacitors: Characterization and Modeling at Both High and Low Temperatures

Zeineb Chabrak Payet, Alexandre De Bernardinis, Pascal Venet, and Richard Lallemand

Abstract The lithium-ion capacitor is a recent energy storage component. Although it has been commercialized for several years, its hybridization still requires further investigation to characterize it. The literature has studied some of its characteristics focusing on experimentation at positive temperatures. This paper aims to enlarge the tests to include very low temperatures, showing the difference between Nyquist plots at 65 and $-30\,°C$. It also presents the Ragone plot for several temperatures, with a comparison between three storage systems: a battery, a supercapacitor, and the lithium-ion capacitor. Finally, a model of the LIC is proposed, for low and high temperatures, with experimental validation.

1 Introduction

With the emergence of applications requiring increasing energy storage systems (ESSs), there is a growing need to study and develop new ones. ESSs can be found in almost every application, from transportation with hybrid and electrical means of transport, to renewable energy sources with photovoltaic and wind turbine firms, all requiring ESSs to store the produced energy.

The mostly known storage components are the battery, with its different compositions, and the supercapacitor or the electrochemical double layer capacitor (EDLC). These components have been deeply studied in literature and their use is widely spread in all the applications. Recently, a new component came to surface and even

Z. Chabrak Payet (✉) · A. De Bernardinis · R. Lallemand
Systèmes et Applications des Technologies de l'Information et de l'Energie, ENS Paris-Saclay, CNRS, Université Paris-Saclay, IFSTTAR, Versailles, France
e-mail: zeineb.chabrak@ifsttar.fr; alexandre.de-bernardinis@ifsttar.fr; richard.lallemand@ifsttar.fr

P. Venet
Univ Lyon, Université Claude Bernard Lyon 1, Ecole Centrale de Lyon, INSA Lyon, CNRS, Ampère, Lyon, France
e-mail: pascal.venet@univ-lyon1.fr

if it has been commercialized for several years now, his use is still not frequent and the studies about it are still limited. This component is the lithium-ion capacitor (LIC), a combination between a lithium-ion battery (LIB) and a supercapacitor (SC).

The lithium-ion capacitor combines a negative electrode from the battery, composed of graphite pre-doped with lithium-ions Li+, and a positive electrode from the supercapacitor, composed of activated carbon. This allows the LIC to acquire a higher energy density than the SC, while conserving a high power density and a long lifetime. The LIC has been commercialized by several manufacturers, but only few are available on the market, like JSR Micro and YUNASKO. The difference between the LICs of the two manufacturers is the capacitance and the type of electrodes.

Some applications started to take place, showing the important impact the LIC could have. Two types of applications could be found in the literature. The first one is the use of LICs in renewable energy, for example, to replace the classic capacitor in a DC bus, to ameliorate the power output of a wind turbine [1]. The second type is the use of LICs in transportation, mainly public transport whether they are on-board of an electric bus or in stationary, on the wayside of a tramway line to save the energy from braking and restore it to the vehicles during accelerations [2].

In the literature, recent papers about this component have been published. They are mainly trying to characterize and model this component in different ways. For the modeling, the first trials were about building a model of a LIC similar to that of a supercapacitor developed in [3] and [4]. But these models were not suitable to all constrains, which is normal since the role of the battery-type electrode in the model cannot be neglected. Other models were established, using electrical components (R and C) and the temperature effect, but they do not take into account the frequency [5]. As for the thermal modeling, it can be found in [6].

Other studies on characterizing this new component focused on the aging tests that are necessary to estimate its lifetime. Lately, this has been studied in [7]. The authors of the paper used a type of LIC with no specified names but with characteristics different from those of the JSR Micro, the mostly known LIC constructor. In [8] and [9], the aging of the LICs from JSR Micro is studied in floating mode and in cycling, confirming the long lifetime of the component.

In all the studies mentioned above, the LIC has always been characterized at positive high temperatures. The experiments in low temperatures are very rare and are limited to a simple Nyquist plot if existing.

This research aims at closing the gap in the characterization of the LIC. We present some new characteristics that, as far as we know, have not been considered in existing literature. The frequency and time domain characterizations will be reproduced, but, rather than focusing only on the positive temperatures, the study will go throughout all the operating temperature range of the LIC, i.e., from -30 to 65 °C. The time domain characterization will allow to plot, for the first time, the Ragone diagram of the LIC for several temperatures, including the lower ones, as far as the discharge current can go. Then, in order to compare those plots, Ragone diagrams of a Li-ion battery and a supercapacitor of nearly the same capacitance

will be plotted as well. Afterwards, a model based on the frequency characterization will be introduced and tested to confirm its accuracy, also for all temperatures range.

2   Experimental Procedure

The experimental part has been performed on two types of prismatic cells of LIC from the same manufacturer, JSR Micro: ULTIMO 2300F ULR and ULTIMO 3300F LR, their characteristics are presented in Table 1. The results of the next sections are those of the LIC 3300F only, since they are almost the same for the two types.

This type of LIC is composed of a positive electrode of activated carbon similar to a supercapacitor's electrode. The negative one is composed of graphite pre-doped with Li-ions Li+, similar to a Li-ion battery's electrode. The electrolyte between the electrodes is an organic one, similar to that of a Li-ion battery, composed of a $LiPF_6$ salt. This hybrid composition given in Fig. 1 increases the energy density of the LIC while keeping a high power density.

The study in this paper concerns only this one type of lithium-ion capacitors, and can be generalized to all cells with the same composition of electrodes. Since other types of LICs exist with completely different electrodes (two electrodes, both with lithium and carbon, for example), they cannot be included in the general results of this paper.

2.1   In Frequency Domain

The characterization in frequency domain is mainly based on electrochemical impedance spectroscopy (EIS), performed using an IM6 Zahner workstation. This technique allows to determine the different electrochemical processes happening inside the cell while applying a small perturbation of voltage or current over a specified frequency range.

Table 1   Characteristics of JSR Micro LICs

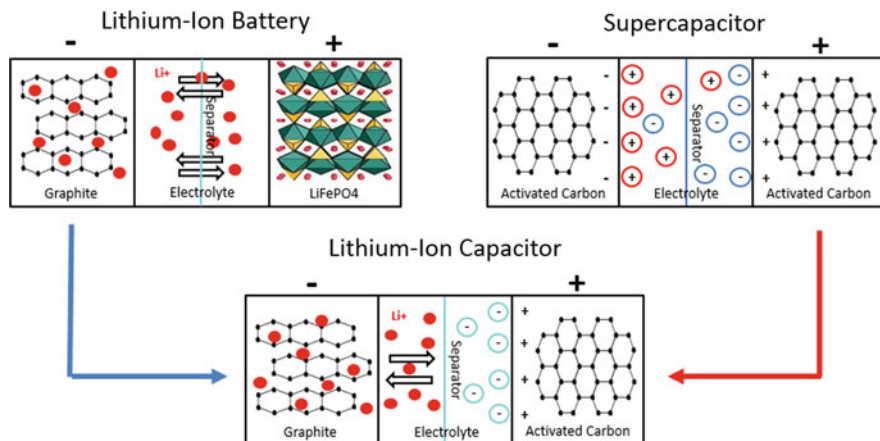| Measurement	Ultimo 2300F ULR	Ultimo 3300F LR
Temperature range	$-30\ldots70\,°C$	$-30\ldots70\,°C$
Voltage range	$2.2\ldots3.8\,V$	$2.2\ldots3.8\,V$
Capacitance	2300 F	3300 F
Resistance at 1 kHz	$0.6\,m\Omega$	$0.7\,m\Omega$
Energy density	8 Wh/Kg	13 Wh/Kg
Weight	0.365 kg	0.350 kg

Fig. 1 Internal composition of the LIC cell

EIS measurements are applied on the LIC for temperatures going from -30 to 65 °C (temperatures of the climatic chamber). The LIC cell stays overnight in the climatic chamber ESPEC at the defined temperature and tests are completed the next day. As for the voltage, measurements are applied for five different voltages (i.e., different states of charge, SoC): 2.2, 2.6, 3, 3.4, and 3.8 V. The galvanostatic mode (fixed current value) has been used to measure the impedance, with an AC maximum current amplitude equal to 5 A. The scanning frequency varied between 10 mHz and 100 kHz.

2.2 In Time Domain

The characterization in time domain is based on a simple charge/discharge process. This has been done using a home-made test-bench with a maximum charge current of 18.9 A and a discharge current up to 400 A. The same temperatures as for frequency domain tests have been selected. The LIC has been charged and discharged fully, i.e., between 2.2 and 3.8 V even if the LIC is theoretically able to accept current up to 1100 A or more [10] for 25 °C, discharge current amplitudes used for tests raised from 10 to 400 A when temperature constrains allow it (since high current amplitudes were impossible to apply for very low temperatures).

3 Results and Discussion

3.1 Ragone Plot

The characterization in time domain has allowed to determine the gravimetric energy and power densities of the Li-Ion capacitor. These densities are needed to plot the Ragone diagram, highly used to compare the performances of different storage systems for a given application regarding their position on the plot. In literature, the existing Ragone diagrams showing the new features of the LIC, i.e., high gravimetric energy density compared to an EDLC and high gravimetric power density compared to a Li-ion battery, are global diagrams plotted at 20 °C, giving only an approximate position of each component. The aim of this section is to plot Ragone diagram of the LIC, with measured values, not only for the usual temperature, but throughout all the possible temperatures. This way, the plotted diagram is more precise and gives indication on the nature of the LIC that have not been observed yet.

The following equations have been used to calculate the peak gravimetric power and the gravimetric energy densities, only for the discharge part, for every discharge current.

- Gravimetric peak power density: $P = max(\frac{VI}{M})$
  P is the gravimetric power density in W/kg, V the voltage in V, I the current in A and M the weight in kg.
- Gravimetric energy density: $E = \frac{\int VIdt}{3600*M}$
  E is the gravimetric energy density in Wh/kg.

3.1.1 Ragone Plot for LIC 3300 F

Figure 2 represents the Ragone diagram for all tested temperatures on a LIC3300F cell. As it can be seen, for high temperatures, the energy density of the LIC is quite high (13 Wh/kg) and the difference between the plots at 25, 45, and 65 °C is almost nonexistent. When temperature decreases, the energy density drops, especially for high discharge current, starting from 10 °C, while the power density stays almost constant. For negative temperatures, the energy density of the LIC becomes very low. The cell cannot be discharged at high currents anymore (maximum current discharge 100 A at −30 °C).

The gravimetric power density does not change a lot with the temperature decrease when remaining over 0 °C. Indeed, the calculation protocol takes into account a constant discharge current, and the peak voltage, which is always near 3.8 V, since the resistance at those temperatures is still small. When evolving towards lower temperatures, the resistance increases considerably, leading to a more significant voltage drop, which results in a much smaller peak voltage at the
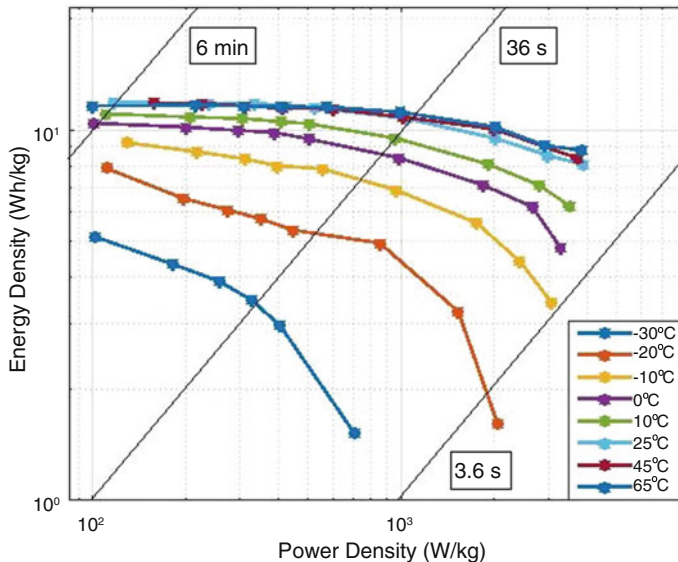
Fig. 2 Ragone diagram of a LIC 3300F at all tested temperatures

beginning of the discharge. This can explain the reason of the decrease of the power density at low temperatures.

To explain the energy density's drop at low temperatures, the LIC will be considered as a thermodynamic system. This way, the energy is equal to the ΔG, the Gibbs energy, with ΔG proportional to $V_p - V_n$. V_p is the potential of the positive electrode, it is the one responsible of the global potential of the cell. V_n is the potential of the negative electrode. For usual temperatures, it is very low and constant, it barely participates in the total cell polarization. This is explained in [11] where authors added a third lithium-reference electrode to study the potentials of the positive and the negative electrodes versus lithium one. When going toward low temperatures, it has been found that the potential of the negative electrode rises significantly, and its contribution to the cell polarization becomes quite important, while the positive electrode's potential remains constant. This results in a decrease of the difference between the two potentials, leading to a smaller ΔG and consequently, a drop in the energy density.

Those results have been confirmed from an electrochemical point of view in [12], where authors studied the electrodes separately to observe the inner processes that take place at low temperatures.

3.1.2 Comparison Between LIC, Battery, and Supercapacitor

The same tests of charge/discharge described above have also been performed for a battery of 1.1 Ah and a supercapacitor of 3000 F. Ragone diagrams of these components have been plotted the same way as the LIC, using the same equations to calculate their gravimetric power and energy densities.

– For the battery: since the maximum current allowed is 30 A, the discharge has been performed for 1, 5, 10, 20, and 30 A. Also, since the maximum temperature is 60 °C, the maximum applied temperature chosen was 45 °C to compare with the other cells.
– For the supercapacitor: the discharge currents applied are the same as those applied to the LIC with also the same temperatures.

Figure 3 shows Ragone diagrams for all three components at four different temperatures -10, 0, 25, and 45 °C, one color for each one. As it can be noticed, a significant gap exists between the energy density of the battery compared to the other cells, with 83 Wh/kg at 25 °C. On the contrary, its power density is quite insufficient, knowing that the power densities of the LIC and the supercapacitor could be much higher since the maximum allowed currents could not be attained, due to the experimental test bench design.
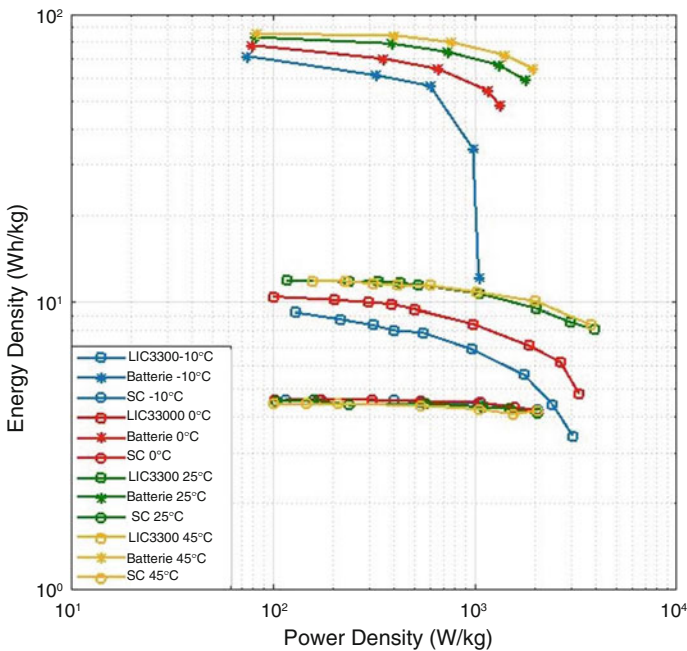

Fig. 3 Ragone diagram for the 3 cells at several temperatures

When comparing the LIC and the supercapacitor, the energy density of the LIC cell is found to be twice the EDLC's one, with also a higher power density for the same current. The difference is that the supercapacitor presents very stable diagrams that barely change with temperature. It is capable of providing the same specific energy at 65 and $-30\,°C$ without any degradation. In contrary, LIC is much more sensitive to the temperature gradient. Indeed, its specific energy decreases a lot and can even reach values smaller than those of the supercapacitor at very low temperature.

From this comparison, it is clear that, for high temperatures, the LIC has inherited the supercapacitor's characteristics, with a higher energy density. However, when the temperature drops, it behaves more like a battery, since the contribution of the negative graphite electrode increases at those temperatures.

3.2 Nyquist Plot

The Nyquist plot is obtained from EIS measurements, and it represents the opposite of the imaginary part of the impedance of the cell as a function of its real part. This plot is a good starting point to determine the inner electrochemical processes happening in the LIC, considering the results in the existing literature.

At high frequencies, the cell has an inductive behavior that will not be discussed below. Only the positive part of -Im(Z) of the plot will be studied, representing the capacitive part.

3.2.1 At Low Temperatures

The Nyquist plots represented in Fig. 4 at low temperatures exhibit at $-30\,°C$ a large semi-circle at medium frequencies, similar to batteries. It represents the charge transfer in the cell, and its radius is proportional to the charge transfer resistance. For a LIC, the charge transfer happens only at the negative electrode, where the oxydo-reduction reaction takes place. It consists of the de-solvation of the lithium ions, their transport into the solid /electrolyte interface and their reduction in charge (the opposite process happens in discharge) [13]. The radius of the semi-circle diminishes when going toward $0\,°C$, since the charge transfer resistance decreases a lot with high temperatures.

After the semi-circle, at low frequencies, a vertical line appears, representing the solid-state diffusion into the active material (graphite) of the electrode, which is, in general, the slowest process in charge or discharge.
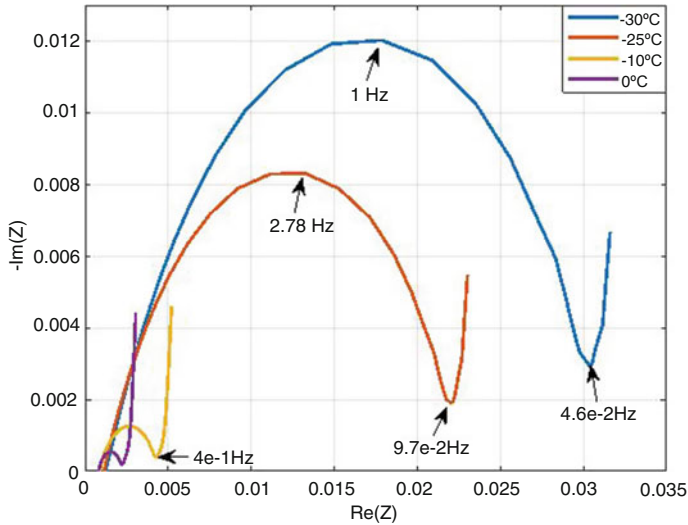
Fig. 4 Nyquist plot at low temperatures for V=3.8V

3.2.2 At High Temperatures

Temperature will be considered as high when it is positive. In the Nyquist plots at high temperatures represented in Fig. 5, it can be noticed that the semi-circles present at low temperatures have disappeared, and they have been replaced by a straight line. In [14], authors explain that the kinetics of the negative graphite electrode tend to be faster than the kinetics of the positive electrode at high temperatures which could explain the form of the Nyquist plot, alike a supercapacitor's plot. The diffusion part remains the same.

3.3 Capacitance vs Voltage

The plot of the capacitance in function of the voltage in Fig. 6 has been calculated from the EIS measurements, where the considered capacitance is taken at the lowest frequency of the Nyquist, i.e., at 10 mHz. In the literature, some papers [15] have mentioned the particularity of this plot for a lithium-ion capacitor, since it shows a minimum of the capacitance at 3 V at positive temperatures. When going towards low temperatures, this particularity begins to disappear and the capacitance tends to vary almost linearly to the voltage above $-10\,°C$, resembling to a supercapacitor's C=f(V) plot. This shows that the participation of the negative electrode in the total capacitance of the LIC can be neglected at low temperatures, and the behavior of the total cell becomes almost identical to a supercapacitor. Knowing that the capacitance of a Li-ion battery decreases sharply with negative temperatures, the result from the plot seems adequate.
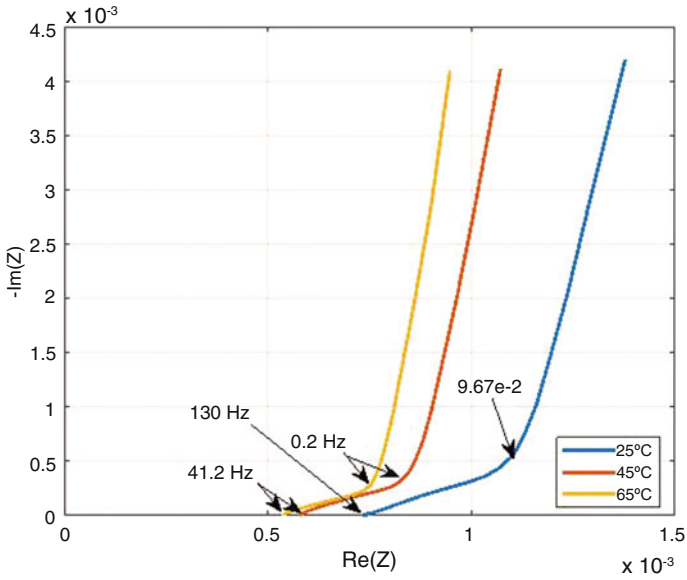
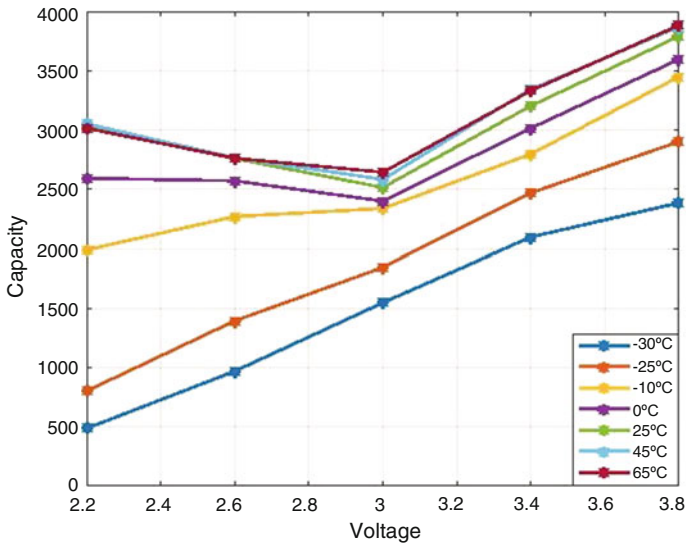**Fig. 5** Nyquist plot at high temperatures for V = 3.8 V

Fig. 6 Capacitance vs voltage for tested temperatures

3.4 Modeling and Test

3.4.1 Model

The elaborated model is mainly based on the electrochemical impedance spectroscopy (EIS) measurements detailed in a previous section. From the Nyquist plots obtained, the internal phenomena have been determined based on the plots of batteries and supercapacitors in the literature.

This model, represented in Fig. 7, is composed of:

- a resistance R_0, at the intersection of the plot with the real axis, when the imaginary part is equal to zero. It represents the ohmic resistance of the cell.
- a constant phase element CPE_1 (Q_1 and n_1) in parallel of a resistance R_1, to model the interfacial phenomenon happening in the cell at medium frequencies. It represents the charge transfer.
- a second constant phase element CPE_2 (Q_2 and n_2) representing the diffusion process happening at low frequencies.

The inductive part at high frequencies is not represented, since it is independent of the temperature and the voltage.

The analytic function of the model is equal to the total impedance Z_{tot} of the cell:

$$Z_{tot} = R_0 + \frac{R_1}{1 + R_1 Q_1 (jw)^{n_1}} + \frac{1}{Q_2 (jw)^{n_2}} \tag{1}$$

To optimize the function above, the ZfitGUI function has been used. It is an open source Matlab function specially designed for Nyquist plots. The function permits to optimize the real and the imaginary part at the same time to determine the best values for the circuit's components, so that the optimized plot fits the best the measured plot with the smallest residue.

Simulations performed as mentioned show good results and fit accurately the experimental data for almost all temperatures. Only for -10 and $0\,°C$, the residual error is more important at the low frequency part. The results are illustrated in Fig. 8, for both temperatures -25 and $45\,°C$.

Indeed, even if Nyquist plots at low and high temperatures are quite different, all processes happening inside the cell remain the same, but their contribution is more or less significant with temperature variations. In the Table 2, values of all the

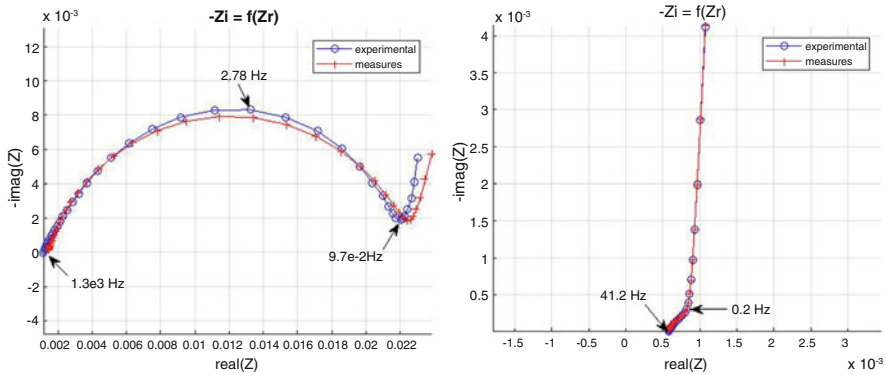**Fig. 7** Equivalent model of LIC in frequency domain
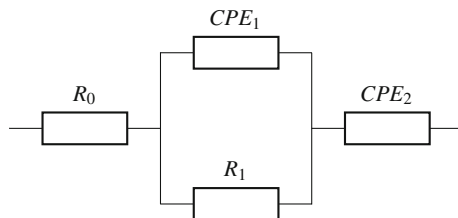
Fig. 8 Experimental and optimized plots at −25 and 45 °C

Table 2 Values of the model parameters obtained by simulation

	−25 °C	−10 °C	0 °C	25 °C	45 °C	65 °C
R0	1.41e−3	9.52e−4	8.53e−4	7.43e−4	5.77e−4	5.62e−4
Q1	3.86	5.19	5.33	1.22e3	1.12e3	1.29e3
n1	0.81	0.83	0.86	0.73	0.83	0.88
R1	2.12e−2	3.25e−3	1.29e−3	3.67e−4	2.88e−4	2.06e−4
Q2	1.87e3	1.59e3	1.58e3	3.30e3	3.51e3	3.54e3
n2	0.85	0.67	0.62	0.95	0.96	0.97

variables have been listed for all temperatures. As it can be seen, for Q1 and Q2 which represent mostly the charge transfer and the diffusion, their values decrease with the decrease of temperature, which confirm the fact that these processes go slower at low temperatures. In the contrary, resistances' values tend to be higher at low temperature, confirming results from EIS measurements.

4 Conclusions

Our results support that the lithium-ion capacitor presents interesting characteristics. For instance, this storage component has inherited some functions from the battery and the supercapacitor, while its hybridization generates new features, as explained in the above. In fact, the difference between all forms of the Nyquist plot at both high and low temperature is a very interesting feature, proving that the behavior of the cell evolves a lot with temperatures. Moreover, the EIS measurements show that the plot of the capacitance vs the voltage of the cell presents a new aspect with a minimum at 3 V that disappears at low temperatures. To our knowledge, this study is first to introduce this result. Experiments at both low and high temperatures

show interesting different results that need to be deeply investigated in further publications, since they are very promising for future applications of the LIC.

References

1. G. Mandic, A. Nasiri, E. Ghotbi, E. Muljadi, Lithium-Ion capacitor energy storage integrated with variable speed wind turbines for power smoothing. IEEE J. Emerg. Select. Topics Power Electron. **1**(4), 287–295 (2013)
2. F. Ciccarelli, A. Del Pizzo, D. Iannuzzi, Improvement of energy efficiency in light railway vehicles based on power management control of wayside lithium-ion capacitor storage. IEEE Trans. Power Electron. **29**(1), 275–286 (2014)
3. S. Barcellona, F. Ciccarelli, D. Iannuzzi, L. Piegari, Modeling and parameter identification of lithium-ion capacitor modules. IEEE Trans. Sustainable Energy. **5**(3), 785–794 (2014)
4. N. El Ghossein, A. Sari, P. Venet, A lithium-ion capacitor electrical model considering pores size dispersion, in *2018 IEEE International Conference on Industrial Technology (ICIT)* (2018)
5. Y. Firouz, N. Omar, J-M. Timmermans, P. Van den Bossche, J. Van Mierlo, Lithium-ion capacitor - characterization and development of new electrical model. Elsevier Energy **83**, 597–613 (2015)
6. Y. Firouz, N. Omar, P. Van den Bossche, J. Van Mierlo, Electro-thermal modeling of new prismatic lithium-ion capacitors, in *2014 IEEE Vehicle Power and Propulsion Conference (VPPC)* (2014)
7. M. Uno, A. Kukita, Cycle life evaluation based on accelerated aging testing for lithium-ion capacitors as alternative to rechargeable batteries. IEEE Trans. Ind. Electron. **63**(3), 1607–1617 (2016)
8. N. El Ghossein, A. Sari, P. Venet, Accelerated cycle aging tests applied to lithium-ion capacitors, in *2017 IEEE Vehicle Power and Propulsion Conference (VPPC)* (2017)
9. N. El Ghossein, A. Sari, P. Venet, Effects of the hybrid composition of commercial lithium-ion capacitors on their floating aging, in *2018 IEEE Transactions on Power Electronics*(2018)
10. J. Ronsmans, B. Lalande, Combining energy with power: lithium-ion capacitors, in *2015 International Conference on Electrical Systems for Aircraft, Railway, Ship Propulsion and Road Vehicles (ESARS)* (2015)
11. P.H. Smith, T.N. Tan, T.L. Jiang, J. Chung, Lithium-ion capacitor: electrochemical performance and thermal behavior. Elsevier J. Power Sources **243**, 982–992 (2013)
12. J. Zhang, J. Wang, Z. Shi, Z. Xu, Electrochemical behavior of lithium ion capacitor under low temperature. J. Electroanalyt.l Chem. **817**, 195–201 (2018)
13. T. Richard Jow, S.A. Delp, J.L. Allen, J-P. Jones, M.C. Smart, Factors limiting Li+ charge transfer kinetics in Li-ion batteries. J. Electrochem. Soc. **165**(2), A361–A367 (2018)
14. M.C.Smart, J.F.Whitacre, B.V.Ratnakumar, K.Amine, Electrochemical performance and kinetics of Li1+x(Co1/3Ni1/3Mn1/3)1xO2 cathodes and graphite anodes in low-temperature electrolytes. J. Power Sources **168**(2), 501–508 (2007)
15. N. El Ghossein, A. Sari, P. Venet, Interpretation of the particularities of lithium-ion capacitors and development of a simple circuit model, in *2016 IEEE Vehicle Power and Propulsion Conference (VPPC)* (2016)